Transl. Stroke Res. (2011) 2:524–532
DOI 10.1007/s12975-011-0130-0

REVIEW ARTICLE

Advances in MRI-Based Detection of Cerebrovascular Changes after Experimental Traumatic Brain Injury

Rick M. Dijkhuizen

Received: 14 September 2011 / Revised: 25 October 2011 / Accepted: 26 October 2011 / Published online: 12 November 2011

Abstract Traumatic brain injury is a heterogeneous and multifaceted neurological disorder that involves diverse pathophysiological pathways and mechanisms. Thorough characterization and monitoring of the brain's status after neurotrauma is therefore highly complicated. Magnetic resonance imaging (MRI) provides a versatile tool for in vivo spatiotemporal assessment of various aspects of central nervous system injury, such as edema formation, perfusion disturbances and structural tissue damage. Moreover, recent advances in MRI methods that make use of contrast agents have opened up additional opportunities for measurement of events at the level of the cerebrovasculature, such as blood–brain barrier permeability, leukocyte infiltration, cell adhesion molecule upregulation and vascular remodeling. It is becoming increasingly clear that these cerebrovascular alterations play a significant role in the progression of post-traumatic brain injury as well as in the process of post-traumatic brain repair. Application of advanced multiparametric MRI strategies in experimental, preclinical studies may significantly aid in the elucidation of pathomechanisms, monitoring of treatment effects, and identification of predictive markers after traumatic brain injury.

Keywords Animal models · Contrast agents · Magnetic resonance imaging · Neuroinflammation · Traumatic brain injury

R. M. Dijkhuizen (✉)
Biomedical MR Imaging and Spectroscopy Group,
Image Sciences Institute, University Medical Center Utrecht,
Building Nieuw Gildestein, Yalelaan 2,
3584 CM Utrecht, The Netherlands
e-mail: rick@invivonmr.uu.nl

Introduction

Magnetic resonance imaging (MRI) is a versatile modality for in vivo imaging of the central nervous system (CNS). The technique relies on detection of MR signals from the highly abundant water protons in tissues. Its versatility stems from the ability to sensitize MRI acquisitions to distinct parameters, such as proton density, MR relaxation times (T_1, T_2), susceptibility contrast, diffusion, perfusion and flow. This enables multiparametric imaging studies on different pathophysiological events that are involved in the evolution of CNS injury, e.g., after neurotrauma. Furthermore, the availability of MRI in hospital and laboratory settings facilitates the translation between clinical and preclinical research. Hence, MRI studies in experimental models of CNS injury can contribute to the characterization of pathomechanisms and treatment effects, which may lead to improvements in diagnosis and therapeutic strategies after CNS injury.

MRI of Tissue and Perfusion Status

MRI in animal models of traumatic brain injury and other CNS diseases most often involve T_2-, diffusion- and/or perfusion-weighted imaging to measure changes in brain tissue and perfusion status (for a review, see Dijkhuizen and Nicolay [1]). The transverse relaxation time of the MR signal, T_2, is dependent on the interstitial water content and increases when intercellular or vasogenic edema develops. This has been demonstrated with T_2-weighted MRI in rats in the first days after controlled cortical impact injury [2–5], closed-head injury [6, 7] and lateral fluid percussion injury [8]. While T_2-weighted MRI serves as a reliable tool to determine the extent and location of CNS lesions at

subacute and chronic stages, earlier tissue changes may be detected with diffusion-weighted MRI. Reduction of the apparent diffusion coefficient (ADC) or diffusivity of tissue water, most likely reflective of cytotoxic cell swelling [9], has been detected within hours after experimental traumatic brain injury, which precedes severe tissue damage, e.g., loss of cellularity, and resultant ADC elevations at later stages [6–8, 10–12]. Furthermore, with diffusion tensor imaging [13], it has been shown that changes in diffusion anisotropy and axial diffusivity in gray and white matter can inform on the extent of pericontusional and diffuse axonal injury after controlled cortical impact in mice [14] and head acceleration in rats [15], respectively. These studies reported permanent loss of diffusion anisotropy and initial decline, followed by rise of diffusivity, which correlated with axonal degeneration and demyelination.

The combination of T_2- and/or diffusion-weighted MRI with perfusion-weighted MRI allows concurrent assessment of tissue lesions and perfusion alterations. Two perfusion-weighted MRI strategies that are frequently applied are dynamic susceptibility contrast (DSC)-enhanced MRI and arterial spin labeling (ASL) [16–18]. DSC MRI allows calculation of various hemodynamic parameters from MR signal changes caused by first passage of an intravascular bolus of contrast agent. ASL is based on spatially selective inversion or saturation of incoming arterial spins and subsequent detection of labeled blood water in perfused tissue, which enables quantification of cerebral blood flow. Both methods have been applied in rodent models of traumatic brain injury, and have provided insights into the development of focal as well as global post-traumatic cerebral hypoperfusion [7, 11, 19–22]. Figure 1 demonstrates how multiparametric MRI can inform on the spatiotemporal profile of tissue and perfusion changes after experimental traumatic brain injury. T_2, diffusivity and cerebral blood flow (CBF) maps, acquired in studies by Immonen et al. [8] and Hayward et al. [20, 23], reveal first signs of secondary injury which slowly evolves from the primary contusion site at a subacute stage after lateral fluid percussion injury in rats, eventually resulting in an enlarged lesion at chronic stages.

Post-traumatic Cerebrovascular Changes

Abovementioned conventional MRI strategies allow depiction of edema formation and perfusion disturbances, which can be useful for diagnosis and treatment evaluation after traumatic brain injury. Nevertheless, the pathophysiology of neurotrauma is highly heterogeneous and complex, and involves various primary and secondary neuropathological pathways [24, 25]. In particular, increasing evidence points towards a major role for inflammatory events in the development of secondary tissue damage following traumatic brain injury, while inflammation has also been implicated in post-traumatic regenerative processes [26–29]. Associated cerebrovascular changes, such as blood–brain barrier (BBB) breakdown, upregulation of cell adhesion molecules, leukocyte infiltration and vascular remodeling, may strongly contribute to secondary hypoperfusion and edema formation after the primary insult, but might also play a part in post-traumatic tissue repair mechanisms [25, 27, 30, 31]. Elucidation of such pathways may contribute to improvement of assessment of injury severity, prediction of lesion progression and identification of targets for interventions after traumatic brain injury. The following paragraphs will briefly describe how specific contrast-enhanced MRI strategies may aid in gaining insights in abovementioned events in relation to neurotrauma.

MRI of BBB Permeability

Assessment of BBB integrity with MRI is based on detection of leakage of MR contrast agent from vascular into parenchymal space in CNS tissue [32, 33]. Intravenously administered paramagnetic contrast agent that leaks out and accumulates in brain parenchyma when microvascular barriers are disrupted, will result in local changes in MR signal intensity. The most frequently used contrast media are gadolinium-containing compounds, such as Gd-DTPA chelate, that locally shorten the longitudinal relaxation time, T_1, of the MR signal. Contrast agents are usually injected as a bolus; however, step-down infusion may improve contrast enhancement through higher contrast agent concentrations in plasma and tissue [34]. Contrast-enhanced BBB permeability imaging usually involves a static approach, in which T_1-weighted MRI is executed at a specific time-point (typically 10–30 min) after contrast agent injection, to detect hyperintense signal intensities generated by extravasated contrast agent. This is a fast, simple and sensitive method, but it merely provides qualitative information on the integrity of the BBB. Quantification of BBB leakage is feasible with dynamic contrast-enhanced (DCE) imaging, involving repetitive T_1-weighted MR image acquisition, and analysis with a tracer kinetic model to assess contrast agent concentration changes in tissue and vasculature as a function of time [33]. This allows calculation of the blood-to-tissue volume transfer constant, K_i or K^{trans}, as well as other parameters, such as the extravascular extracellular space volume. Analytical approaches that are frequently applied include Tofts' compartmental analysis [35] and multiple time-graphic, or Patlak plot analysis [36]. Quantification of BBB permeability with these analysis methods, however, relies on certain physiological assumptions that may not

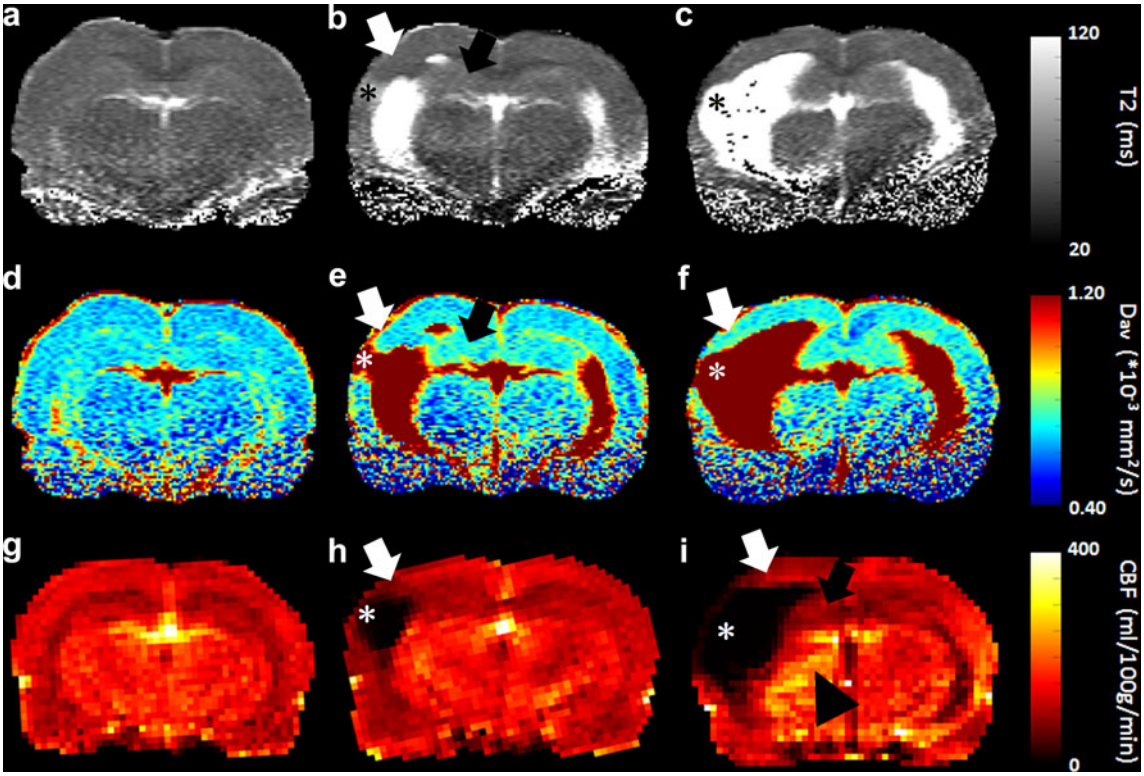

Fig. 1 Maps of T_2 (**a**–**c**), D_{av} ('average diffusivity' = 1/3 of the trace of the diffusion tensor) (**d**–**f**), and CBF (**g**–**i**) of a coronal brain slice from control rats (*left column*), and rats at 2–3 weeks (*middle column*) and 8 months after lateral fluid percussion injury (*right column*). Data are acquired from a quantitative MRI study by Immonen et al. [8] (**a** and **d**, **b** and **e**, and **c** and **f** are map pairs from the same animal, respectively) and CBF studies by Hayward et al. [20, 23], executed on a 4.7-T MR system with quadrature surface coil as radio-frequency transmitter/receiver (for T_2 and D_{av} mapping), or a combination of an actively decoupled linear volume transmission coil and quadrature surface receiver (for CBF mapping with ASL). The parametric MRI maps demonstrate that at the cortical contusion site (*), a lesion/cyst was formed which slowly expanded (together with enlarging ventricles) up to several months post-injury. The perilesional cortical area (*white arrows*) and remaining tissue in the hippocampus ipsilateral to the contusion site (*black arrows*) show gradual increase in T_2 and diffusivity from 2 to 3 weeks post-injury onwards, indicative of progression of neurodegeneration (acute alterations in T_2 and diffusivity during the first week post-injury are edema-related and resolved by 2 weeks; data not shown). CBF was decreased in the perilesional area and in the ipsilateral hippocampus 2 weeks post-injury, and remained lowered 8 months later. At this chronic stage increased CBF is apparent in the ipsilateral thalamus (*arrowhead*). Scale bar = 1 mm (Courtesy of Drs. Riikka Immonen, Nick Hayward and Olli Gröhn)

invariably hold under pathological conditions, for instance because of deviations in vascular delivery and cellular uptake of the tracer.

Serial BBB permeability MRI studies, particularly in cerebral ischemia–reperfusion models, have provided evidence for early and late BBB breakdown after experimental CNS injury [37–39]. However, the exact temporal profile of BBB permeability changes is still unclear, as studies include reports of persistent [39], as well as biphasic BBB opening [38]. Acute, transient BBB leakage, as detected with post-contrast T_1-weighted MRI, has been shown after experimental traumatic brain injury, and may be prolonged by a post-traumatic secondary insult [40, 41]. In rabbits with weight-drop induced traumatic brain injury, serial DCE MRI revealed increasing K^{trans} in the focal lesion area from 3 h to 3 days post-trauma [42] (Fig. 2). This was followed by a gradual decline, but K^{trans} remained elevated up to 30 days as compared to animals with sham injury.

MRI of Leukocytes

Cellular MRI is based on the detection of cells that have been labeled with MR contrast agent, such as paramagnetic chelates, superparamagnetic particles or ^{19}F MRI-detectable fluorinated particles (for reviews, see Modo et al. [43] and Stoll and Bendszus [44]). MRI-based visualization of various types of hepatobiliary, hematopoietic, immune and stem cells, has most frequently relied on labeling with superparamagnetic iron oxides [43]. These particles, generally ranging in size from a few nanometers to more than a micrometer, can induce very strong contrast effects by local shortening of the T_2 or T_2^*, resulting in hypointense signal

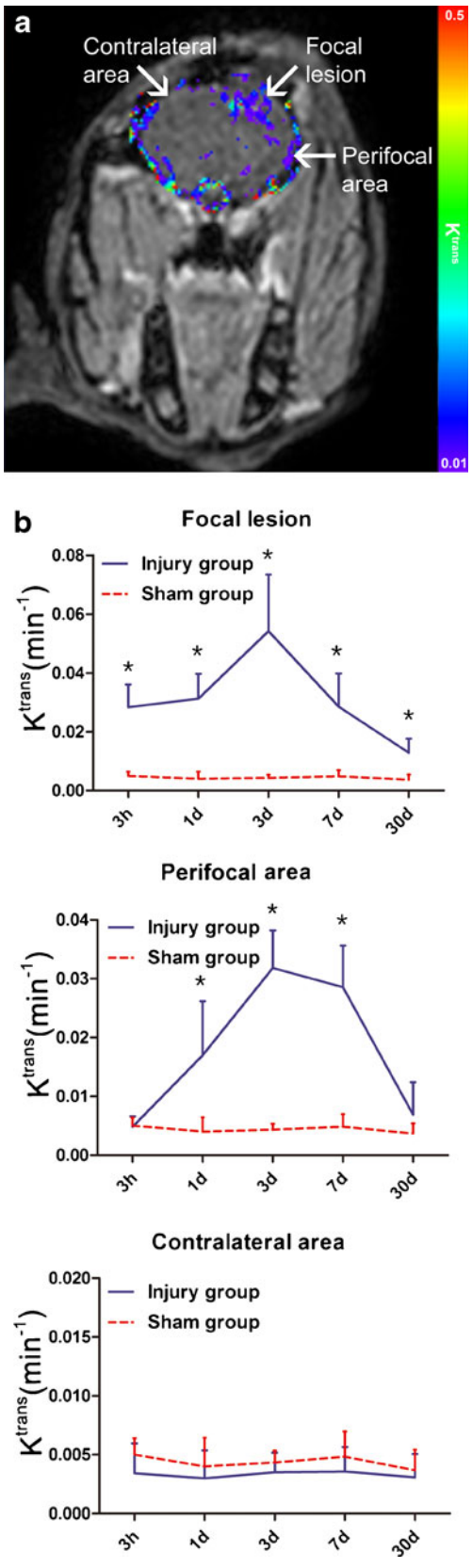

Fig. 2 K^{trans} map (**a**) derived from DCE MRI of rabbit brain 3 days after weight drop induced traumatic brain injury [42]. BBB permeability is increased in focal and perifocal lesion areas as compared to contralateral. Graphs (**b**) show K^{trans} in different brain areas over time after traumatic brain injury or sham injury. In the focal lesion area (*top graph*), K^{trans} was consistently higher than in comparable brain regions of sham-operated animals from 3 h up to 30 days after traumatic brain injury, peaking around day 3. In the perifocal area (*middle graph*), K^{trans} was higher at 1, 3 and 7 days post-trauma, as compared to the sham group. In contralateral brain tissue (*bottom graph*), K^{trans} was similar in the traumatic brain injury and sham injury groups at all time-points. Exact details of the location and size of the regions-of-interest are described by Wei et al. [42]. Data represent mean ± SD. $^{*}P<0.01$ as compared to the sham group. The publisher for part of this copyrighted material is Mary Ann Liebert, Inc. publishers (Courtesy of Dr. Xiao-Er Wei)

intensity on T_2- (spin echo) or T_2^*-weighted (gradient echo) MR images. Basically two approaches for cellular labeling have been employed: (1) in vivo uptake of intravenously injected contrast agent by (circulating) phagocytic cells or (2) in vitro labeling of isolated cells that are subsequently reinjected. Ultrasmall particles of iron oxide (USPIOs) with a long blood half-life have been mostly applied for in vivo uptake by monocytes or macrophages, whereas larger particles of iron oxide (such as small particles of iron oxide (SPIOs) or micron-sized particles of iron oxide (MPIOs)), which provide maximum contrast effects, may be effectively used for in vitro cell labeling [43, 44]. Both cell labeling strategies have been applied in a number of experimental studies that sought to characterize the spatiotemporal profile of leukocyte infiltration in neuroinflammatory diseases, such as multiple sclerosis and stroke (see Stoll and Bendszus [44] and references therein). These studies have, for instance, shown that cellular infiltration is not necessarily linked to BBB disruption. In a controlled cortical impact injury model in mice, intravenous MPIO injection resulted in discrete, punctuate areas of MRI hypointensity in and around contusion sites (see Fig. 3), which correlated histologically with presence of MPIO-containing macrophages [45]. This was evident even when MPIOs were administered 6 days before neurotrauma, which suggests that previously labeled macrophages migrate to the trauma site and that the hypointense MR signals were not caused by nonspecific accumulation of MPIO particles that traversed an acutely leaky BBB.

MRI of Cell Adhesion Molecules

Advances in design and synthesis of contrast agents have recently initiated MRI studies that take advantage of molecular targeting with tailored contrast agents to measure particular disease markers [46–49]. This kind of molecular imaging with MRI typically employs (super)paramagnetic nano- or microparticles with conjugated ligand, e.g., an antibody. Beside a (super)paramagnetic agent, e.g., gadolinium

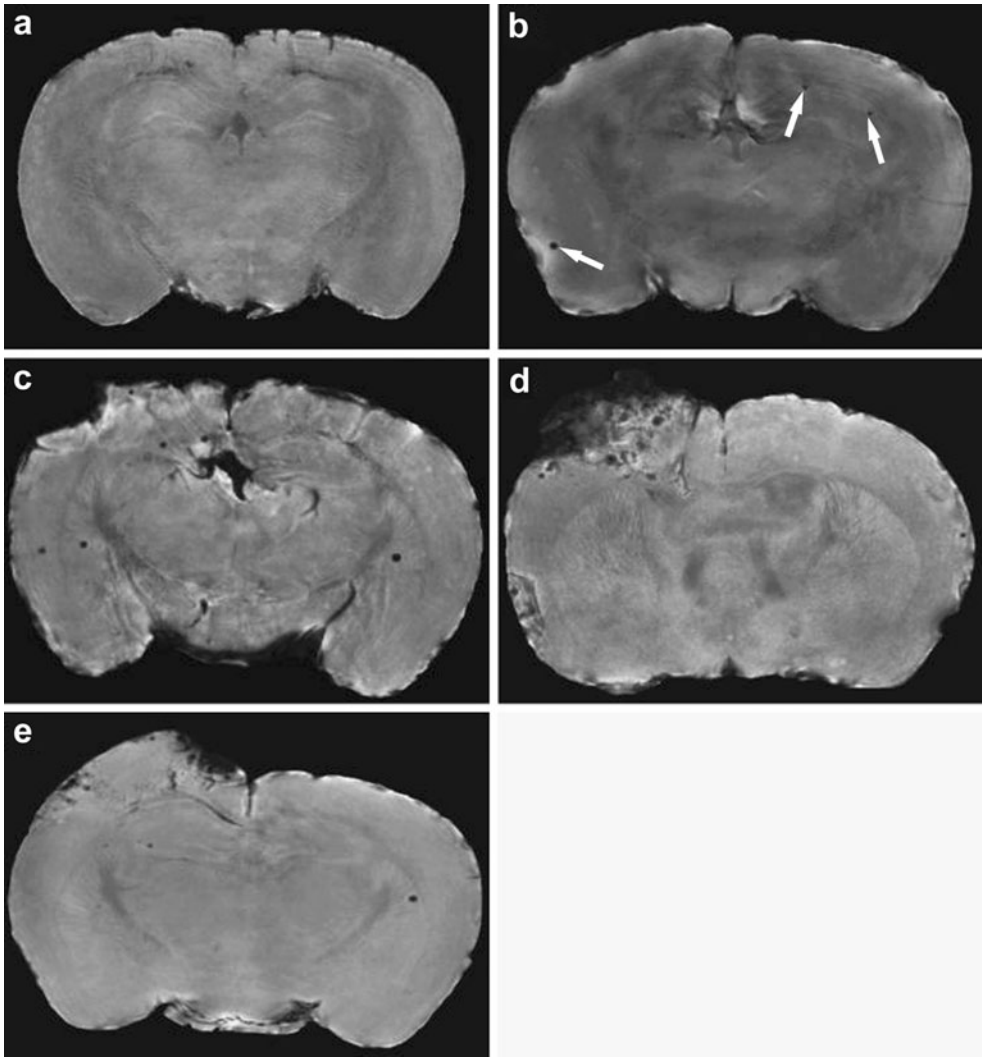

Fig. 3 High-resolution T_2^*-weighted MR images (acquired with a 11.7-T MR system) of coronal sections of excised brain from: **a** a naive mouse with no contrast injection; **b** a naive mouse that was injected 24 h earlier with MPIO particles; **c** a mouse injected with MPIO particles at 24 h and imaged at 48 h after controlled cortical impact injury; **d** a mouse injected with MPIO particles at 48 h and imaged at 72 h after controlled cortical impact injury; **e** a mouse injected with MPIO particles at 6 days before and imaged at 48 h after controlled cortical impact injury (from Foley et al. [45]). A low level of randomly localized areas of punctuate hypointensity (*arrows*) representing MPIO particles was identified after injection of MPIO particles in naive mice (**b**). More robust contusional and peri-contusional accumulation of particles was found in mice injected with MPIO particles after controlled cortical impact injury (**c**, **d**), particularly when particles were injected at 48 h post-trauma and imaged 24 h thereafter (**d**). Smaller numbers of particles were observed in mouse brain at 48 h post-trauma when MPIO particles were injected 6 days prior to traumatic brain injury (**e**). The publisher for this copyrighted material is Mary Ann Liebert, Inc. publishers

or iron oxide, particles may contain other labels, such as fluorescent dye, for detection with alternative imaging modalities. In addition, polyethylene-glycol coating is often used to increase circulation time and bioavailability.

Molecular MRI contrast agents can be constructed by direct functionalization of (super)paramagnetic agents or particles (e.g., MPIOs) with targeting peptides or antibodies [50]. An alternative platform for the design and formation of molecular imaging probes makes use of lipid formulations, such as liposomes and micelles, that are build up from amphiphilic lipids [51] (Fig. 4). These lipid-based structures can carry various contrast agents in relatively high amounts, which, in combination with the ease of preparation, flexibility and biocompatibility, make these nanoparticles highly adequate for preclinical cellular and molecular imaging studies as well as for drug delivery in patients [52].

Despite the potential of targeted contrast agents to bind and depict molecular markers, molecular MRI studies in the brain are complicated due to the presence of the BBB, which restricts the blood-to-brain transfer of relatively large intravascular molecular MRI probes. For that reason

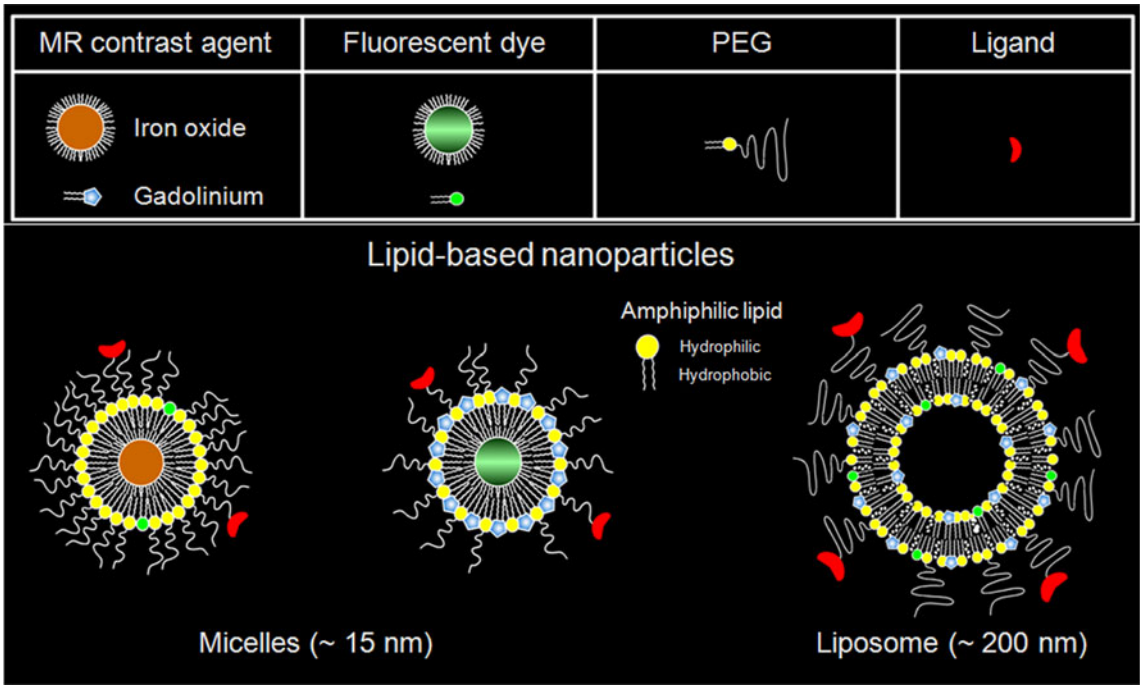

Fig. 4 Schematic representation of two types of lipid-based nanoparticles, i.e., micelles and liposomes, that can be formed with various constituents, such as MR contrast agent, fluorescent dye, polyethylene-glycol (PEG), and a targeting ligand for molecular imaging purposes. Courtesy of Drs. Geralda A. van Tilborg and Willem J. Mulder

molecular MRI in CNS injury models have largely focused on detection of markers that are expressed on the luminal side of cerebral blood vessels, such as cell adhesion molecules. Studies in rodent models of neuroinflammatory diseases have demonstrated that paramagnetic or superparamagnetic compounds targeted against endothelial cell adhesion molecules, such as P- and E-selectin and VCAM-1, induce local contrast enhancement on T_1- or T_2^*-weighted MR images, respectively, reflective of activated cerebral endothelium [53–56]. In a model of lateral fluid percussion in rats, Chapon et al. [57] recently showed that injection of selectin-targeted iron oxide particles resulted in persistent T_2^* shortening in the traumatized brain hemisphere, while initial T_2^* shortening recovered within 1 h after injection of non-targeted iron oxide particles.

MRI of Vascularity

There is increasing evidence that chronic vascular remodeling can occur after CNS injury, which may contribute to

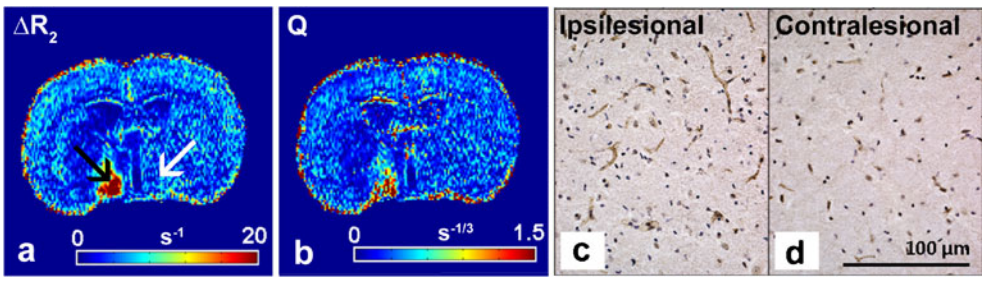

Fig. 5 ΔR_2 (**a**) and Q map (**b**) calculated from steady-state contrast-enhanced MRI of a coronal rat brain slice with a subcortical infarct at 7 days after transient unilateral middle cerebral artery occlusion, and corresponding histological sections with vessel staining of the ipsi- (**c**) and contralesional hypothalamic region (**d**). Relatively high ΔR_2 after administration of a superparamagnetic blood pool agent (USPIO) indicates a high density of microvessels with a relatively small diameter in the ipsilesional hypothalamic region (*black arrow*) as compared to contralesional (*white arrow*) (**a**). This area also revealed a high *Q* value (**b**), reflective of enhanced microvessel density, which was confirmed by more vessel staining with von Willebrand Factor (DAB-enhanced; brown) in the ipsi- (**c**) as compared to contralesional hypothalamic region (**d**) (nuclei were stained with hematoxylin; blue). Modified from Seevinck et al. [59] (Courtesy of Peter R. Seevinck, Lisette H. Deddens and H. Elga de Vries)

reestablishment of perfusion, removal of waste product or tissue repair [31, 58]. Preclinical studies have reported traumatic brain injury-induced angiogenesis, which could be promoted with specific therapeutic interventions, leading to improvement of functional outcome [31]. Hayward et al. [23] have recently detected brain region-specific increases in vascular density at 9 months after lateral fluid percussion injury in rats, which, however, showed no clear correlation with restoration of CBF or recovery of neurological function. Evidently, the pattern of changes in brain tissue vascularity and its relation to pathophysiology or plasticity after neurotrauma require further investigation.

Various MRI methods are available for detection of vascular changes in injured brain (for a review, see Seevinck et al. [59]). A particularly powerful approach is offered by steady-state contrast-enhanced MRI, which involves concurrent gradient echo and spin echo MRI acquisition in combination with injection of a superparamagnetic blood pool agent (e.g., USPIOs). This enables measurement of changes in MR relaxation rates R_2^* and R_2 that are dependent on local cerebral blood volume (CBV), which allows calculation of different vascular parameters, such as total and microvascular blood volume fraction, microvessel density, and vessel size index [59, 60]. A serial steady state contrast-enhanced MRI study in rats after experimental stroke has reported chronically increased microvascular CBV and microvessel density subsequent to subacute vascular compression, pointing toward active revascularization of post-ischemic tissue [61]. Figure 5 shows steady state contrast-enhanced MRI data obtained from a rat at 7 days after subcortical stroke. The elevated ΔR_2 (a measure of microvascular CBV) and Q $(\Delta R_2/(\Delta R_2^*)^{2/3}$; a measure of microvessel density) in part of the lesion reflect increased vascularization, which was confirmed histologically [59].

Conclusion

Recent MRI strategies that focus on detection of specific cerebrovascular alterations associated with neurological disorders have advanced the abilities of integrative in vivo studies on the pathophysiology of CNS injury. In particular, the developments in contrast agent chemistry have provided unique opportunities for in vivo MRI-based detection of cellular and molecular processes at the level of the cerebrovasculature, such as the invasion of leukocytes and upregulation of cell adhesion molecules. The application of these cellular and molecular MRI methods in combination with other structural and functional MRI techniques, allows direct correlation of different pathophysiological events in an experimental setting, which can contribute to elucidation of the interaction between the various pathways through which traumatic brain injury develops. Furthermore, preclinical experiments with multiparametric MRI protocols may lead to the identification of exclusive disease biomarkers and distinctive therapeutic targets that can be translated to the clinic. The potential of advanced MRI techniques, such as susceptibility-weighted MRI and diffusion tensor imaging, to aid in the classification of traumatic brain injury patients has recently been described by Kou et al. [62]. These methods, in combination with functional MRI, may also inform on brain remodelling or neural plasticity at later post-traumatic stages [63], which could lead to identification of key processes that contribute to functional recovery and may be stimulated with therapeutic strategies.

In conclusion, studies with novel contrast-enhanced MRI strategies in animal models will provide more insights into the potential of these methods in terms of their sensitivity and specificity to detect distinctive characteristics of traumatic brain injury. The outcome of such studies, as well as adequate evaluation of safety issues, will be critical to determine whether these contrast-enhanced MRI techniques have potential for clinical application in neurotrauma patients.

Acknowledgements Research leading to this paper has received funding from the Netherlands Organization for Scientific Research (NWO) (VIDI 917.76.347) and the European Union's Seventh Framework Programme (FP7/2007-2013) under grant agreements no. 201024 and no. 202213 (European Stroke Network).

References

1. Dijkhuizen RM, Nicolay K. Magnetic resonance imaging in experimental models of brain disorders. J Cereb Blood Flow Metab. 2003;23:1383–402.
2. Kochanek PM, Marion DW, Zhang W, Schiding JK, White M, Palmer AM, et al. Severe controlled cortical impact in rats: assessment of cerebral edema, blood flow, and contusion volume. J Neurotrauma. 1995;12:1015–25.
3. Obenaus A, Robbins M, Blanco G, Galloway NR, Snissarenko E, Gillard E, et al. Multi-modal magnetic resonance imaging alterations in two rat models of mild neurotrauma. J Neurotrauma. 2007;24:1147–60.
4. Schuhmann MU, Stiller D, Skardelly M, Mokktarzadeh M, Thomas S, Brinker T, et al. Determination of contusion and oedema volume by MRI corresponds to changes of brain water content following controlled cortical impact injury. Acta Neurochir Suppl. 2002;81:213–5.
5. Unterberg AW, Stroop R, Thomale UW, Kiening KL, Pauser S, Vollmann W. Characterisation of brain edema following "controlled cortical impact injury" in rats. Acta Neurochir Suppl. 1997;70:106–8.

6. Assaf Y, Beit-Yannai E, Shohami E, Berman E, Cohen Y. Diffusion- and T2-weighted MRI of closed-head injury in rats: a time course study and correlation with histology. Magn Reson Imaging. 1997;15:77–85.
7. Assaf Y, Holokovsky A, Berman E, Shapira Y, Shohami E, Cohen Y. Diffusion and perfusion magnetic resonance imaging following closed head injury in rats. J Neurotrauma. 1999;16:1165–76.
8. Immonen RJ, Kharatishvili I, Niskanen JP, Grohn H, Pitkanen A, Grohn OH. Distinct MRI pattern in lesional and perilesional area after traumatic brain injury in rat—11 months follow-up. Exp Neurol. 2009;215:29–40.
9. Moseley ME, Cohen Y, Mintorovitch J, Chileuitt L, Shimizu H, Kucharczyk J, et al. Early detection of regional cerebral ischemia in cats: comparison of diffusion- and T2-weighted MRI and spectroscopy. Magn Reson Med. 1990;14:330–46.
10. Albensi BC, Knoblach SM, Chew BG, O'Reilly MP, Faden AI, Pekar JJ. Diffusion and high resolution MRI of traumatic brain injury in rats: time course and correlation with histology. Exp Neurol. 2000;162:61–72.
11. Pasco A, Lemaire L, Franconi F, Lefur Y, Noury F, Saint-Andre JP, et al. Perfusional deficit and the dynamics of cerebral edemas in experimental traumatic brain injury using perfusion and diffusion-weighted magnetic resonance imaging. J Neurotrauma. 2007;24:1321–30.
12. Van Putten HP, Bouwhuis MG, Muizelaar JP, Lyeth BG, Berman RF. Diffusion-weighted imaging of edema following traumatic brain injury in rats: effects of secondary hypoxia. J Neurotrauma. 2005;22:857–72.
13. Basser PJ, Mattiello J, LeBihan D. MR diffusion tensor spectroscopy and imaging. Biophys J. 1994;66:259–67.
14. Mac Donald CL, Dikranian K, Bayly P, Holtzman D, Brody D. Diffusion tensor imaging reliably detects experimental traumatic axonal injury and indicates approximate time of injury. J Neurosci. 2007;27:11869–76.
15. Li J, Li XY, Feng DF, Gu L. Quantitative evaluation of microscopic injury with diffusion tensor imaging in a rat model of diffuse axonal injury. Eur J Neurosci. 2011;33:933–45.
16. Barbier EL, Lamalle L, Decorps M. Methodology of brain perfusion imaging. J Magn Reson Imaging. 2001;13:496–520.
17. Calamante F, Thomas DL, Pell GS, Wiersma J, Turner R. Measuring cerebral blood flow using magnetic resonance imaging techniques. J Cereb Blood Flow Metab. 1999;19:701–35.
18. Zaharchuk G. Theoretical basis of hemodynamic MR imaging techniques to measure cerebral blood volume, cerebral blood flow, and permeability. AJNR Am J Neuroradiol. 2007;28:1850–8.
19. Forbes ML, Hendrich KS, Kochanek PM, Williams DS, Schiding JK, Wisniewski SR, et al. Assessment of cerebral blood flow and CO_2 reactivity after controlled cortical impact by perfusion magnetic resonance imaging using arterial spin-labeling in rats. J Cereb Blood Flow Metab. 1997;17:865–74.
20. Hayward NM, Tuunanen PI, Immonen R, Ndode-Ekane XE, Pitkanen A, Grohn O. Magnetic resonance imaging of regional hemodynamic and cerebrovascular recovery after lateral fluid-percussion brain injury in rats. J Cereb Blood Flow Metab. 2011;31:166–77.
21. Hendrich KS, Kochanek PM, Williams DS, Schiding JK, Marion DW, Ho C. Early perfusion after controlled cortical impact in rats: quantification by arterial spin-labeled MRI and the influence of spin-lattice relaxation time heterogeneity. Magn Reson Med. 1999;42:673–81.
22. Immonen R, Heikkinen T, Tahtivaara L, Nurmi A, Stenius TK, Puolivali J, et al. Cerebral blood volume alterations in the perilesional areas in the rat brain after traumatic brain injury—comparison with behavioral outcome. J Cereb Blood Flow Metab. 2010;30:1318–28.
23. Hayward NM, Immonen R, Tuunanen PI, Ndode-Ekane XE, Grohn O, Pitkanen A. Association of chronic vascular changes with functional outcome after traumatic brain injury in rats. J Neurotrauma. 2010;27:2203–19.
24. Greve MW, Zink BJ. Pathophysiology of traumatic brain injury. Mt Sinai J Med. 2009;76:97–104.
25. Werner C, Engelhard K. Pathophysiology of traumatic brain injury. Br J Anaesth. 2007;99:4–9.
26. Cederberg D, Siesjo P. What has inflammation to do with traumatic brain injury? Childs Nerv Syst. 2010;26:221–6.
27. Lenzlinger PM, Morganti-Kossmann MC, Laurer HL, McIntosh TK. The duality of the inflammatory response to traumatic brain injury. Mol Neurobiol. 2001;24:169–81.
28. Morganti-Kossmann MC, Satgunaseelan L, Bye N, Kossmann T. Modulation of immune response by head injury. Injury. 2007;38:1392–400.
29. Schmidt OI, Heyde CE, Ertel W, Stahel PF. Closed head injury—an inflammatory disease? Brain Res Brain Res Rev. 2005;48:388–99.
30. Shlosberg D, Benifla M, Kaufer D, Friedman A. Blood–brain barrier breakdown as a therapeutic target in traumatic brain injury. Nat Rev Neurol. 2010;6:393–403.
31. Xiong Y, Mahmood A, Chopp M. Angiogenesis, neurogenesis and brain recovery of function following injury. Curr Opin Investig Drugs. 2010;11:298–308.
32. Runge VM, Muroff LR, Wells JW. Principles of contrast enhancement in the evaluation of brain diseases: an overview. J Magn Reson Imaging. 1997;7:5–13.
33. Tofts PS, Brix G, Buckley DL, Evelhoch JL, Henderson E, Knopp MV, et al. Estimating kinetic parameters from dynamic contrast-enhanced T(1)-weighted MRI of a diffusable tracer: standardized quantities and symbols. J Magn Reson Imaging. 1999;10:223–32.
34. Nagaraja TN, Nagesh V, Ewing JR, Whitton PA, Fenstermacher JD, Knight RA. Step-down infusions of Gd-DTPA yield greater contrast-enhanced magnetic resonance images of BBB damage in acute stroke than bolus injections. Magn Reson Imaging. 2007;25:311–8.
35. Tofts PS, Kermode AG. Measurement of the blood–brain barrier permeability and leakage space using dynamic MR imaging: 1. Fundamental concepts. Magn Reson Med. 1991;17:357–67.
36. Ewing JR, Knight RA, Nagaraja TN, Yee JS, Nagesh V, Whitton PA, et al. Patlak plots of Gd-DTPA MRI data yield blood–brain transfer constants concordant with those of 14C-sucrose in areas of blood–brain opening. Magn Reson Med. 2003;50:283–92.
37. Nagaraja TN, Knight RA, Ewing JR, Karki K, Nagesh V, Fenstermacher JD. Multiparametric magnetic resonance imaging and repeated measurements of blood–brain barrier permeability to contrast agents. Methods Mol Biol. 2011;686:193–212.
38. Pillai DR, Dittmar MS, Baldaranov D, Heidemann RM, Henning EC, Schuierer G, et al. Cerebral ischemia–reperfusion injury in rats—a 3T MRI study on biphasic blood–brain barrier opening and the dynamics of edema formation. J Cereb Blood Flow Metab. 2009;29:1846–55.
39. Strbian D, Durukan A, Pitkonen M, Marinkovic I, Tatlisumak E, Pedrono E, et al. The blood–brain barrier is continuously open for several weeks following transient focal cerebral ischemia. Neuroscience. 2008;153:175–81.
40. Barzo P, Marmarou A, Fatouros P, Corwin F, Dunbar J. Magnetic resonance imaging-monitored acute blood–brain barrier changes in experimental traumatic brain injury. J Neurosurg. 1996;85:1113–21.
41. Beaumont A, Marmarou A, Hayasaki K, Barzo P, Fatouros P, Corwin F, et al. The permissive nature of blood brain barrier (BBB) opening in edema formation following traumatic brain injury. Acta Neurochir Suppl. 2000;76:125–9.

42. Wei XE, Zhang YZ, Li YH, Li MH, Li WB. Dynamics of rabbit brain edema in focal lesion and perilesion area after traumatic brain injury: a MRI study. J Neurotrauma. 2011. doi:10.1089/neu.2010.1510.
43. Modo M, Hoehn M, Bulte JW. Cellular MR imaging. Mol Imaging. 2005;4:143–64.
44. Stoll G, Bendszus M. New approaches to neuroimaging of central nervous system inflammation. Curr Opin Neurol. 2010;23:282–6.
45. Foley LM, Hitchens TK, Ho C, Janesko-Feldman KL, Melick JA, Bayir H, et al. Magnetic resonance imaging assessment of macrophage accumulation in mouse brain after experimental traumatic brain injury. J Neurotrauma. 2009;26:1509–19.
46. Lanza GM, Winter PM, Caruthers SD, Morawski AM, Schmieder AH, Crowder KC, et al. Magnetic resonance molecular imaging with nanoparticles. J Nucl Cardiol. 2004;11:733–43.
47. Sosnovik DE, Weissleder R. Emerging concepts in molecular MRI. Curr Opin Biotechnol. 2007;18:4–10.
48. Strijkers GJ, Mulder WJ, van Tilborg GA, Nicolay K. MRI contrast agents: current status and future perspectives. Anticancer Agents Med Chem. 2007;7:291–305.
49. Weissleder R, Mahmood U. Molecular imaging. Radiology. 2001;219:316–33.
50. McAteer MA, Akhtar AM, von Zur Muhlen C, Choudhury RP. An approach to molecular imaging of atherosclerosis, thrombosis, and vascular inflammation using microparticles of iron oxide. Atherosclerosis. 2010;209:18–27.
51. Mulder WJ, Strijkers GJ, van Tilborg GA, Griffioen AW, Nicolay K. Lipid-based nanoparticles for contrast-enhanced MRI and molecular imaging. NMR Biomed. 2006;19:142–64.
52. Torchilin VP. Recent advances with liposomes as pharmaceutical carriers. Nat Rev Drug Discov. 2005;4:145–60.
53. Barber PA, Foniok T, Kirk D, Buchan AM, Laurent S, Boutry S, et al. MR molecular imaging of early endothelial activation in focal ischemia. Ann Neurol. 2004;56:116–20.
54. McAteer MA, Sibson NR, von Zur Muhlen C, Schneider JE, Lowe AS, Warrick N, et al. In vivo magnetic resonance imaging of acute brain inflammation using microparticles of iron oxide. Nat Med. 2007;13:1253–8.
55. Sibson NR, Blamire AM, Bernades-Silva M, Laurent S, Boutry S, Muller RN, et al. MRI detection of early endothelial activation in brain inflammation. Magn Reson Med. 2004;51:248–52.
56. Sipkins DA, Gijbels K, Tropper FD, Bednarski M, Li KC, Steinman L. ICAM-1 expression in autoimmune encephalitis visualized using magnetic resonance imaging. J Neuroimmunol. 2000;104:1–9.
57. Chapon C, Franconi F, Lacoeuille F, Hindre F, Saulnier P, Benoit JP, et al. Imaging E-selectin expression following traumatic brain injury in the rat using a targeted USPIO contrast agent. MAGMA. 2009;22:167–74.
58. Arai K, Jin G, Navaratna D, Lo EH. Brain angiogenesis in developmental and pathological processes: neurovascular injury and angiogenic recovery after stroke. FEBS J. 2009;276:4644–52.
59. Seevinck PR, Deddens LH, Dijkhuizen RM. Magnetic resonance imaging of brain angiogenesis after stroke. Angiogenesis. 2010;13:101–11.
60. Wu EX, Tang H, Jensen JH. Applications of ultrasmall superparamagnetic iron oxide contrast agents in the MR study of animal models. NMR Biomed. 2004;17:478–83.
61. Lin CY, Chang C, Cheung WM, Lin MH, Chen JJ, Hsu CY, et al. Dynamic changes in vascular permeability, cerebral blood volume, vascular density, and size after transient focal cerebral ischemia in rats: evaluation with contrast-enhanced magnetic resonance imaging. J Cereb Blood Flow Metab. 2008;28:1491–501.
62. Kou Z, Wu Z, Tong KA, Holshouser B, Benson RR, Hu J, et al. The role of advanced MR imaging findings as biomarkers of traumatic brain injury. J Head Trauma Rehabil. 2010;25:267–82.
63. Chen H, Epstein J, Stern E. Neural plasticity after acquired brain injury: evidence from functional neuroimaging. PM R. 2010;2:S306–12.